Holographic Lithography for Microcircuits

Ray T. Chen, Lev Sadovnik, Tin M. Aye and Tomasz Jannson

Physical Optics Corporation
2545 West. 237th Street, Suite B
Torrance, CA 90505

ABSTRACT

Experimental results of a high resolution holographic imaging system using lensless geometry are demonstrated. A master mask is imaged on a photopolymer and is recorded as a volume hologram, which is then employed as the holographic mask. Formation of a 0.5 μm resolution image was consistently observed in a large field with illumination by an Argon laser operating at 457 nm, and the pattern was successfully recorded on photoresist.

1. INTRODUCTION

Holographic lithography is still an attractive goal for researchers due to the inexpensive and lensless technology it implies [1] In order to meet the growing requirement for submicron resolution, all holographic aberration should be eliminated [2].However, the diffraction limit has restricted the resolution of a pattern which could be transferred from an original to a hologram. It is well known [3] that the maximum spatial frequency of a sinusoidal component still producing diffracted plan wave in free space is $n \leq 1/\lambda$. In this paper, Argon laser wavelength λ=457.9 nm , which imposes a half-micron resolution limit was employed. Another approach is the use of evanescent wave illumination described in reference 4. Theoretically it seems to be applicable to submicron lithography.

Since Edwin B. Champagne and K.A. Stetson's pioneering work [5,6] there has been continuous interest to improve resolution and signal-to-noise ratios by using TIR hologram. In this paper, we report a volume holographic recording system utilizing a TIR geometry, which initially results in 0.5 micron resolution and signal-to-noise ratio better than 10dB in reconstructed image.

2.EXPERIMENTAL TECHNIQUE

The same arrangement has been used for the recording as well as for the reconstruction process (Figure 1). For the reconstruction, the hologram was rotated through 180 degrees around a perpendicular axis so that the same reference beam could be used as a conjugated beam.

A schematic explanation of the holographic geometry used is shown in figure 2. A transparent object (master mask) when illuminated produces a set of plane waves according to Fourier expansion of the transmittance.

Two sets of interference fringes are generated by each of the object plane waves, for example, as for zero-order harmonic is shown in figure 2. The double fringe structure increases diffraction efficiency as high as 80% and produces a sharp Bragg diffraction peak that can be seen from spectrophotometric measurements (Figure 3). Relatively high absorption of the polymer film [7] that we have employed in our recording would normally produce considerable nonuniformity. But this is compensated for by the advantage of the dry processing. We have not observed any significant shifting of the Bragg diffraction peak in this material during the holographic formation process.

3. SPACER MAINATAINING ACCURACY

It was found both theoretically and experimentally that the most crucial point for submicron resolution holographic lithography is the separation between the object and hologram in recording process, and between the hologram and photoresist plane in reconstruction. The separation distance should be kept exactly the same for both processes.

We know that the spherical aberration could be described by the term

$$\exp\left\{-\frac{i2\pi}{\lambda_o}\frac{\left(x^2+y^2\right)}{8}\,2\left[\frac{\lambda_o}{\lambda_r}\left(\frac{1}{R_i^3}-\frac{1}{R_r^3}\right)+\frac{1}{R_o^3}+\frac{1}{R^3}\right]\right\} \tag{1}$$

Assuming $\lambda_O = \lambda_r = \lambda$, the wavelengths are equal for both steps, and reference and reconstructed beams are plane waves so $R_r=R_o \rightarrow \infty$. Thus, the phase shift due to spherical aberration is:

$$\Delta\Phi = \frac{\pi}{4\lambda}\rho^4\left(\frac{1}{z^3}-\frac{1}{(z+\Delta z)^3}\right) \tag{2}$$

where Δz is the difference from the condition of an equal separation z and $\rho = \sqrt{x^2+y^2}$ is the radius vector in the plane.

The system is practically free of aberrations when the intensity variations at the diffraction focus are less than 20%. This requirement yields

$$|\Delta\Phi| \le (0.2)^{\frac{1}{2}} \tag{3}$$

The effective diameter of the portion of the hologram being transformed into a real image at any one point in the image plane is

$$\rho = z\tan\alpha \tag{4}$$

where $\sin\alpha=\lambda\nu$, from the diffraction equation. This means that the effective diameter of the portion of the hologram participating mainly in image reconstruction depends on the spatial frequency, i.e., resolution, so that

$$\rho = z\frac{\lambda\nu}{(1-\lambda^2\nu^2)^{1/2}} \tag{5}$$

Substituting (4) into (2) and taking (3) we finally obtain

$$\Delta z \le z\left[1-\frac{4(0.2)^{\frac{1}{2}}\lambda}{\pi\tan\alpha\, z}\right]^{-\frac{1}{3}} - z \tag{6}$$

Expanding the last inequality we have

$$\Delta z \le 0.19\frac{\lambda}{\tan^4\alpha} \tag{7}$$

It can be seen from figure 4 that for high resolution (>2μm^{-1}) the separation distance should be kept exactly the same for both processes. Indeed the reproducible result was consistently achieved when a fixed spacer of thickness 50 micron was used for recording and reconstruction.

4. PHOTORESIST IMAGE RECORDING

In order to make present holographic techniques applicable to traditional lithography, a photoresist coated on glass was employed to demonstrate the final pattern. A Shipley AZ-1350J photoresist was chosen (0.85μm thick) and a standard 80% diluted AZ-319A developer was used without the benefit of cleanroom conditions. The photoresist film fabrication included glass cleaning and resist spinning.

The photographs in figure 5 confirm the high resolution capability of the system. Features as small as 0.5μm are resolved. Also, as expected, no geometrical aberrations were observed.

The master mask consisted of an e-beam of 0.5 micron width chromium lines with 1 micron separation on glass substrate. The whole length was 1 inch. The reproduced image kept the ratio of the widths of transparent and opaque parts. Due to the large (1500x) magnification, it was impossible to focus a conventional microscope on the wide field of view. That is why the width of the lines in figure 5 are not uniform.

There were no special precautions taken to avoid dust. Dust is visible in the photograph taken under reflected light.

5. STABILITY PROBLEMS

The TIR hologram was experimentally found to be insensitive to parallel shifting within the illuminated area and rotation within a ±2° range. The latter is in good agreement with Kogelnik's theoretical expression for the dephasing measure [8]

$$\vartheta = \Delta\theta\, K \sin(\phi - \theta_0) - \Delta\lambda\, K^2 / 4\pi n \tag{8}$$

Where K is the grating vector,n is the index of refraction, ϕ is the slant angle and θ_0 is the angle of incidence. The wavelength dispersion $\Delta\lambda$ = 20 nm (half-width of the Bragg peak in figure 3) implies that an angular selectivity

$$\Delta\theta = \frac{\Delta\lambda}{\lambda}\tan(\phi - \theta_0) = 4.5^0 \tag{9}$$

is expected.

This is an extremely important result for future applications since an adjustment of a holographic mask with a reconstruction beam becomes available in a broader range of deviation from the initial (recording) position.

6.CONCLUSION

Summarizing the results presented above, we conclude that a combination of TIR geometry with a new dry processable photo polymer material for volume hologram can provide the capability of holographic microlithography in submicron range. By fixing the distance between holographic plate and image plane, a reproducable aberation free result was achieved. Further theoretical calculation ensures that the technology reported is capable of making large area, submicron lithography. The submicron holographic imaging system is relatively simple and, therefore, the cost is expected to be reduced drastically.

7. ACKNOWLEDGMENTS

The work reported here was supported by the U.S. Air Force Wright Research and Development Center under contract F-33615-89-C-1093.

8. REFERENCES

1. Daniel J. Ehrich and Jeffrey Y. Tsao, Laser Microfabrication, part I, Academic Press Inc, San Diego, CA, 1989.

2. Edwin B. Champagne, "Nonparaxial Imaging Magnification and Aberation Properties in Holography," JOSA, 57, 51-55, 1967.

3. Joseph W. Goodman, Introduction to Fourier Optics, McGraw-Hill, New York, 1968.

4. H. Nassenstein, "Superresolution by Diffraction of Subwaves," Optics Communications, 2, 231-234, 1970.

5. Karl A. Stetson, "Holography With Total Internal Reflected Light," Appl. Phy.Lett 11, 225-226, 1967.

6. Edwin B. Champagne and Norman T. Massey, "Resolution in, Holography," Appl. Opt. 8 , 1879-1885, 1969.

7. B.M. Monroe, W.K. Smouthers, R.R. Krebs, and D.J. Mickish, "Holographic Photopolymers," SPSE Abstracts, 1, 131-135, Wilmington, 1987.

8. H. Kogelnik, "Coupled Wave Theory for Thick Hologram Gratings," Bell System Tech. J. 48, 2909-2947, 1969.

9. L. Sadovnik, "Effect of Finite Size of Periodic Transparencies On the Intensity of Fresnel Images," Opt. Spectrosc 63, 363-367, 1987.

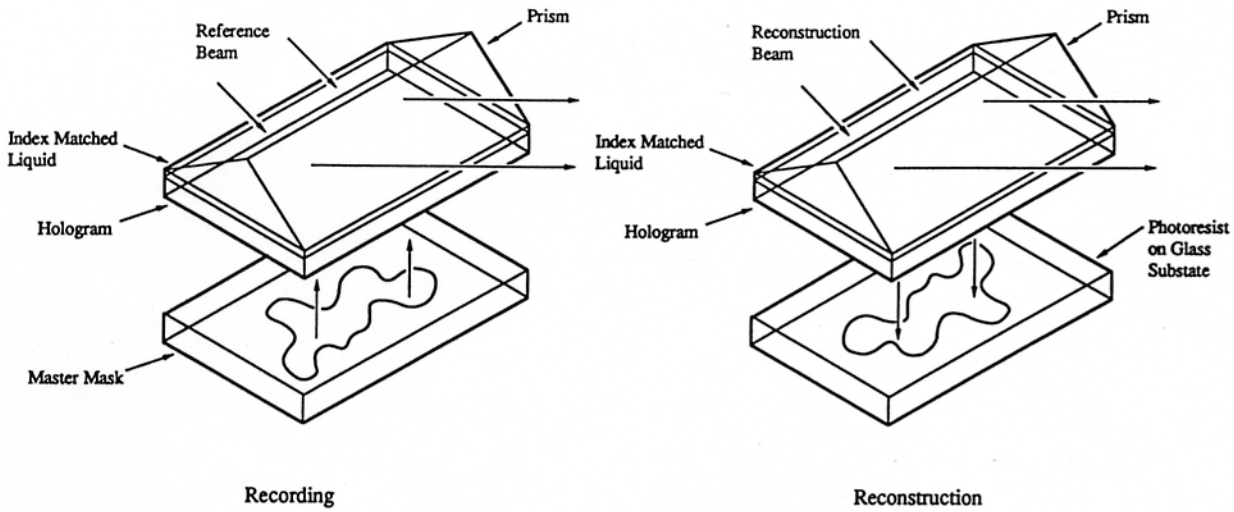

Figure 1 Holographic microlithography with TIR set up.

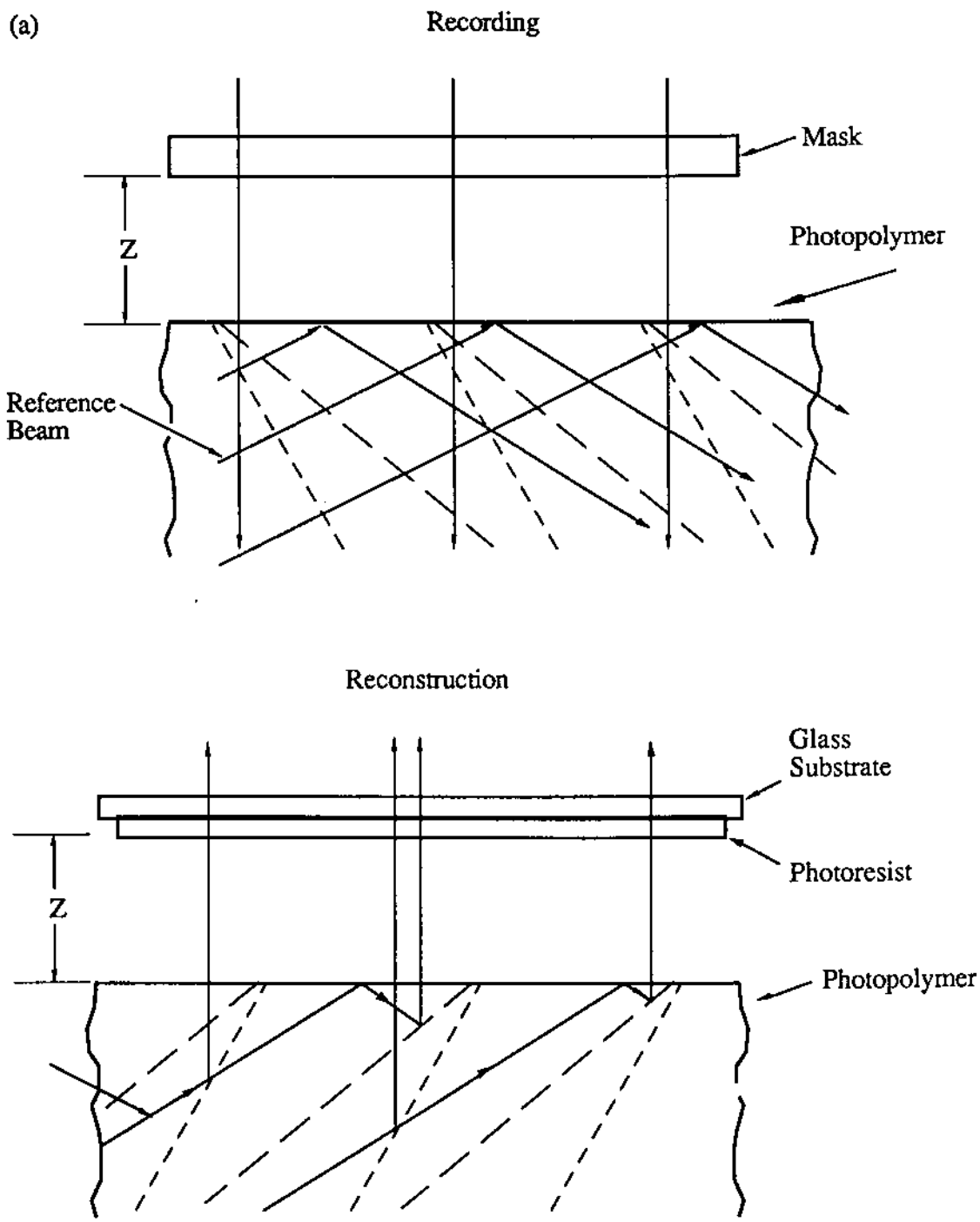

Figure 2 (a) Recording and (b) reconstruction geometries. Two sets of fringes are shown by dashed lines. The hologram has been rotated on 180° for readout.

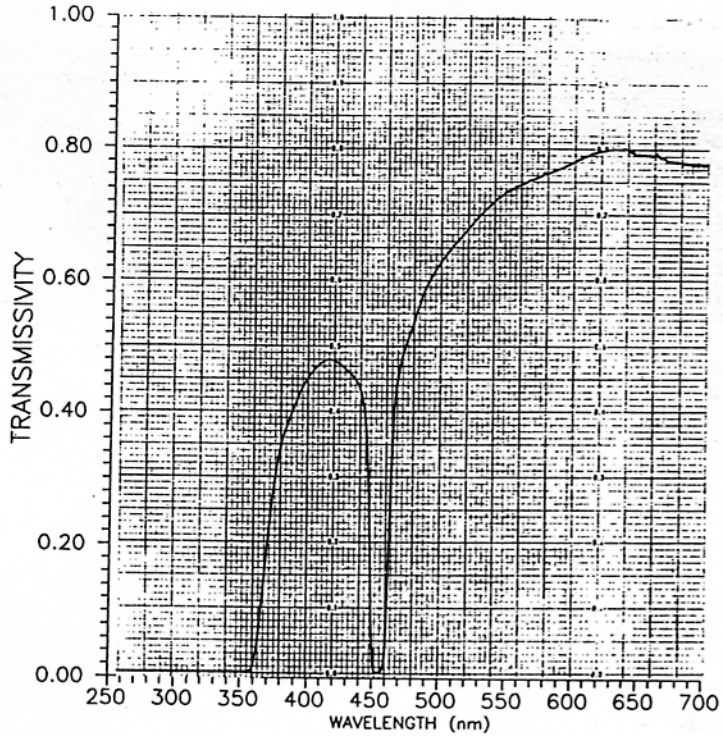

Figure 3 Spectral Transmittance of the Volume Hologram Recorded Without Mask.

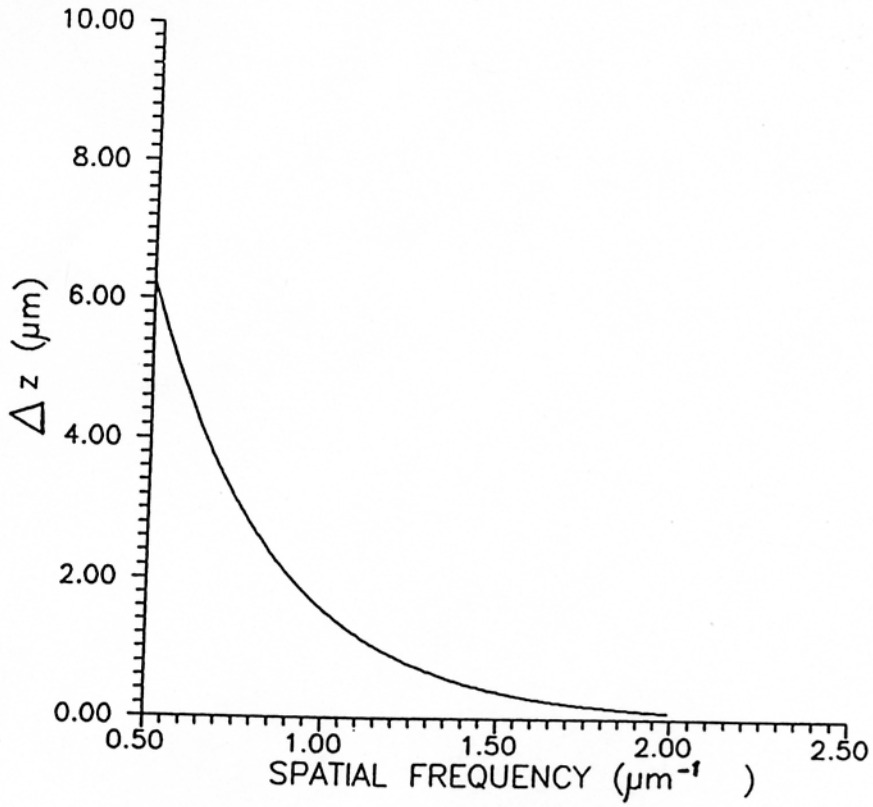

Figure 4 Accuracy of Equal Separations for the Recording and the Reconstruction Process.

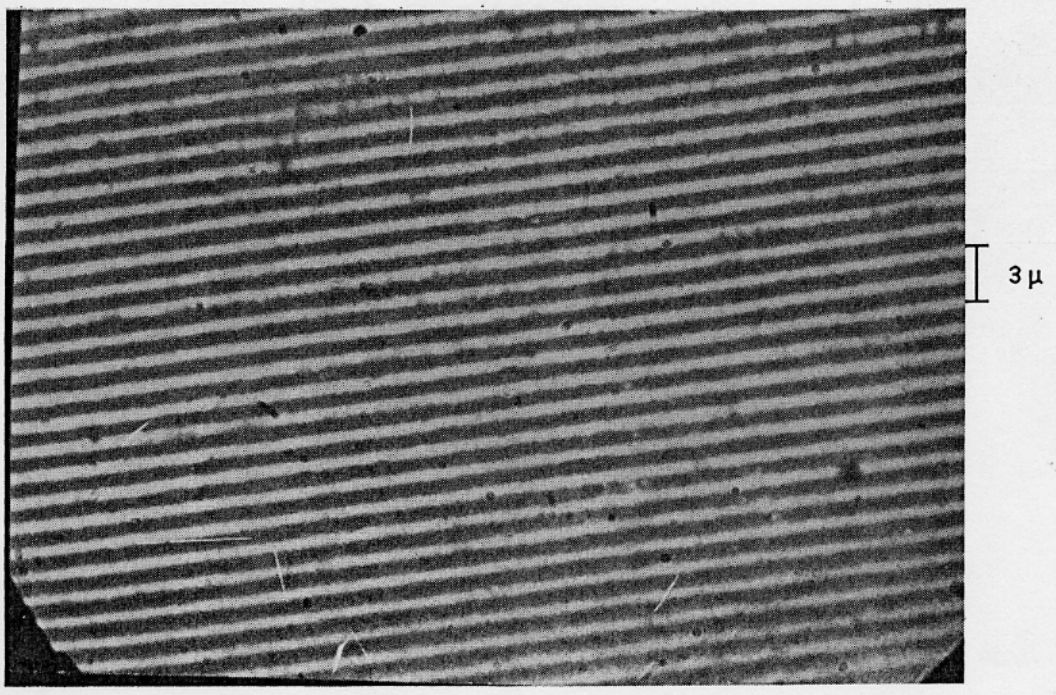

Figure 5 Photograph of the 0.5 micron resolution holographic image recorded on photoresist. Magnification 1500 x.